THE ASTROPHYSICAL JOURNAL, 434:330–340, 1994 October 10

FLAT SPECTRUM T TAURI STARS: THE CASE FOR INFALL

NURIA CALVET[1]
Centro de Investigaciones de Astronomia, Ap. Postal 264, Mérida 5101-A, Venezuela
E-mail: ncalvet@cida.ve

AND

LEE HARTMANN, SCOTT J. KENYON, AND BARBARA A. WHITNEY
Harvard-Smithsonian Center for Astrophysics, Mail Stop 15, 60 Garden Street, Cambridge, MA 02138
E-mail: hartmanncfa.harvard.edu,kenyon@cfa.harvard.edu,bwhitney@cfa.harvard.edu
Received 1993 December 27; accepted 1994 April 12

ABSTRACT

We show that the mid- to far-infrared fluxes of "flat spectrum" T Tauri stars can be explained by radiative equilibrium emission from infalling dusty envelopes. Infall eliminates the need for accretion disks with non-standard temperature distributions. The simplicity and power of this explanation indicates that models employing "active" disks, in which the temperature distribution is a parameterized power law, should be invoked with caution. Infall also naturally explains the scattered light nebulae detected around many flat spectrum sources. To match the observed spectra, material must fall onto a disk rather than the central star, as expected for collapse of a rotating molecular cloud. It may be necessary to invoke cavities in the envelopes to explain the strength of optical and near-infrared emission; these cavities could be produced by the powerful bipolar outflows commonly observed from young stars. If viewed along the cavity, a source may be lightly extincted at visual wavelengths, while still accreting substantial amounts of material from the envelope. Infall may also be needed to explain the infrared-bright companions of many optical T Tauri stars. This picture suggests that many of the flat spectrum sources are "protostars"—young stellar objects surrounded by dusty infalling envelopes of substantial mass.

Subject headings: accretion, accretion disks — infrared: stars — line: formation — stars: pre–main-sequence

1. INTRODUCTION

The paradigm of dusty accretion disks encircling T Tauri stars (Lynden-Bell & Pringle 1974) has been the basis of extensive research over the last decade (Rucinski 1985; Adams, Lada, & Shu 1987, 1988, hereafter ALS I, II; Kenyon & Hartmann 1987, hereafter KH; Bertout, Basri, & Bouvier 1988; Basri & Bertout 1989). Disks appear to be the most plausible explanation of the infrared excesses of many young stellar objects, as well as the millimeter wavelength radio emission (Beckwith et al. 1990). However, most T Tauri stars with infrared excesses emit more radiation at long wavelengths than predicted by the simplest disk theories (KH; ALS II), posing an important challenge to theory.

For many T Tauri stars, such as GG Tau (Fig. 1), the infrared excesses are relatively modest. It is possible that the spectrum of GG Tau can be explained with a slight modification of the basic steady-accretion, flat disk model (shown as a dot-dashed line in Fig. 1). For example, if the disk is slightly curved or "flared" upward, as might be expected from hydrostatic equilibrium, more light from the central star can be absorbed, producing more emission at long wavelengths (KH; dashed line in Fig. 1). However, the "flat spectrum" T Tauri stars pointed out by ALS II, such as HL Tau (Fig. 1), have such large far-infrared excess emission that small modifications to the disk will not suffice to explain the spectrum. Either the heating mechanism must be drastically modified, or another dusty component must be present (Natta 1993).

The spectral energy distribution (SED) of a flat spectrum source implies that much of the luminosity is radiated at large distances, in contrast with simple disk models in which most of the energy is released deep on the gravitational potential well of the system (cf. Lynden-Bell & Pringle 1974; KH; ALS II). Spiral density waves have been invoked to transfer the necessary large amounts of energy to outer disk regions (ALS II; Adams et al. 1989; Shu et al. 1990). Unfortunately, this mechanism may require an unrealistically sharp outer edge to the disk, and predictions of the disk heating by spiral waves have not yet been made.

Other dusty structures have been invoked to explain the excess infrared emission of T Tauri stars. Dusty disk winds emit the excess infrared radiation directly (Safier 1993a, b) or could enhance disk emission by scattering more light from the central star into the disk (Natta 1993). However, the physics of disk winds are uncertain; and if the dust is not well mixed with the gas, it is not clear that the wind (which must arise from the upper layers of the gaseous disk) will necessarily contain much dust.

The largest infrared excesses observed in young stars probably arise in surrounding dusty envelopes rather than in disks. Objects with large far-infrared excesses, known as "Class I" sources in the nomenclature of Lada & Wilking (1984), are thought to be embedded in optically thick, dusty infalling envelopes (Myers et al. 1987; ALS I; Kenyon, Calvet, & Hartmann, 1993a hereafter KCH; Kenyon et al. 1993b, hereafter KWGH). It is plausible that many of these objects are "protostars," used loosely in the sense of young stellar objects which have yet to accrete a substantial amount of their final mass.

In Figure 1 we show the SED of a typical Class I source in the Taurus molecular cloud, IRAS 04016+2610. It is immediately evident that the flat spectrum source HL Tau has a

[1] Also Grup d'Astrofisica de la Societat Catalana de Fisica, Institut d'Estudis Catalans.

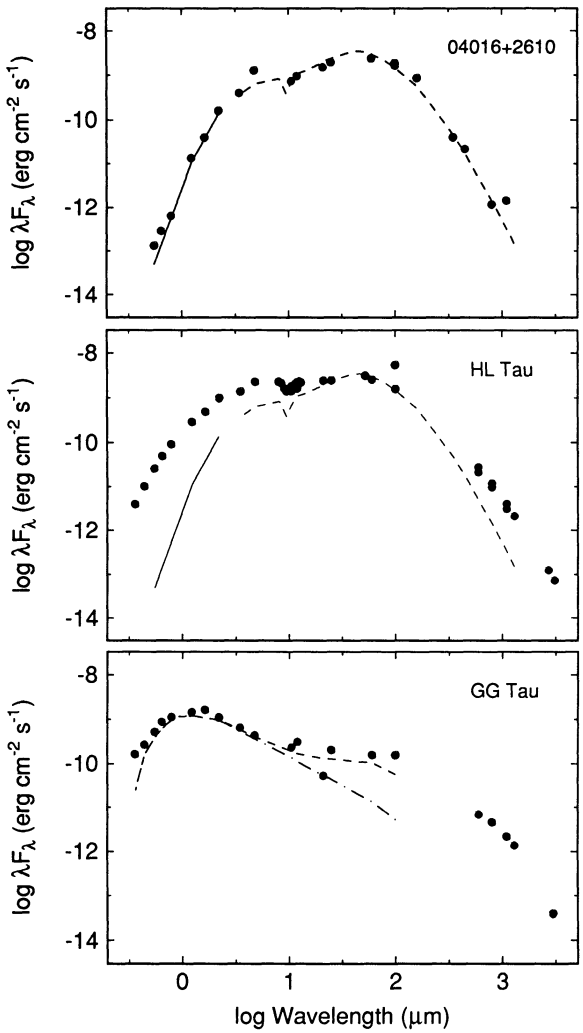

FIG. 1.—Spectral energy distributions (SEDs) of the Class I (protostellar) source 04016+2610 (*upper panel*), the "flat-spectrum" T Tauri star HL Tau (*middle panel*), and the T Tauri star GG Tau. The dashed line in the upper panel represents the dusty infalling envelope model calculated by KCH for 04016+2610. The model has an infall rate of $\dot{M} = 5.7 \times 10^{-6}\ M_\odot\ \mathrm{yr}^{-1} \times (M_c/1\ M_\odot)^{1/2}$, where M_c is the central stellar mass, and a centrifugal radius $R_c = 70$ A.U., observed at an inclination angle $i = 60°$ from the polar axis. The solid line denotes the Monte Carlo scattering calculations of KWGH for this object. The same model is also displayed in the middle panel for comparison with the observations of HL Tau. The dot-dashed line in the bottom panel represents an M0 star plus standard flat disk model. The dashed line represents a "flared" reprocessing disk, with the vertical height H of the disk varying with radial distance r as $H \propto r^{9/8}$ (Kenyon & Hartmann 1987; see text).

SED much closer to that of the Class I source than to the spectrum of the typical T Tauri star. This comparison suggests that the far-infrared emission of HL Tau might also arise from an infalling dusty envelope rather than a disk. Indeed, infall has independently been suggested in HL Tau on the basis of scattered light analyses and high-resolution spectroscopy (Beckwith et al. 1989; Grasdalen et al. 1989), and recently from interferometry at radio wavelengths (Hayashi, Ohashi, & Miyama 1993). ALS II also suggested the presence of a tenuous infalling envelope to explain the far-infrared emission and silicate absorption of HL Tau.

Since infall must eventually cease, one might imagine that Figure 1 can be read from top to bottom as a sort of evolutionary sequence: a young star is first hidden at optical wavelengths by its dusty envelope, then becomes more revealed as the envelope optical depth decreases, and finally emerges as a typical T Tauri star, with perhaps a trace of infall remaining to explain the far-infrared spectrum. Whether or not such an evolutionary sequence can be developed, it is clear that the emission from an infalling envelope can potentially eliminate the need for a disk mechanism to explain the "flat spectrum" temperature distribution.

In this paper we present radiative equilibrium dust envelope models that can explain the spectra of flat spectrum sources, building on our earlier modeling of the Taurus Class I sources (KCH; KWGH). We find that envelope models can explain the mid- to far-infrared emission of flat spectrum sources, although disk emission is probably necessary to explain the observations at the shortest and longest wavelengths. In a subsequent paper we will explore the relationship of infalling envelopes to the overall spectral evolution of T Tauri stars.

2. METHODS AND ASSUMPTIONS

2.1. *Infalling Envelope Models*

Extending the pioneering work of ALS I, KCH and KWGH demonstrated that the SEDs of the Class I sources in Taurus can be explained by the emission of infalling dusty envelopes in radiative equilibrium. The key ingredient in the models is rotation, which causes material to fall directly onto the disk, not the star, reducing the extinction in the inner envelope and allowing more short-wavelength light to escape. The upper panel of Figure 1 demonstrates how well a model of this type can fit the SED of Class I source 04016+2610.

A direct application of this same infall model to HL Tau results in surprisingly good agreement at mid- to far-infrared wavelengths (Fig. 1). Some enhancement of envelope emission is required at shorter wavelengths to match the observations. One possibility is that holes in the envelope are present which allow more short-wavelength radiation to escape; such holes are needed to explain the near-infrared fluxes of Class I sources (KGWH). In addition, the inclusion of disk emission could increase near-infrared fluxes. Here we discuss modifications of our models and radiative equilibrium methods needed to model the optically visible flat spectrum sources.

As in KCH and KWGH, we adopt the Terebey, Shu, & Cassen (1984, hereafter TSC) density distribution for a rotating, infalling envelope. At large distances, the TSC model is in essentially spherical steady free-fall, with a density distribution $\rho \approx r^{-3/2}$. On small scales rotation becomes important, and most of the material lands on a disk rather than directly onto the star. The centrifugal radius R_c denotes the maximum radius to which infalling material lands on the disk at a given instant. The basic TSC model is defined by four parameters: the density at a reference level ρ_1, the centrifugal radius R_c, the total system luminosity L, and the inclination i of the polar (rotational) axis to the line of sight.

For consistency with KCH we define the reference density ρ_1 as that density the model would have at a radius of 1 A.U. if $R_c = 0$. The relationship between ρ_1, the mass infall rate $\dot{M}$, and the stellar mass M_* is

$$\dot{M} = 1.9 \times 10^{-6}\ M_\odot\ \mathrm{yr}^{-1} \left(\frac{\rho_1}{10^{-14}\ \mathrm{g\ cm}^{-3}}\right)\left(\frac{M_*}{1\ M_\odot}\right)^{1/2} . \quad (1)$$

Thus ρ_1 fixes the mass infall rate if the central mass is known.

In KWGH we found that it was impossible to explain the near-infrared emission of Class I sources in Taurus without appealing to scattering in cavities in the dusty infalling envelopes. We suggested that these holes might be driven by the bipolar outflows commonly observed in early evolution (cf. Terebey, Vogel, & Myers 1989). Short wavelength radiation would more easily scatter out of such holes; the solid line in Figure 1 shows a calculation of scattering from an envelope hole. Since objects like HL Tau are known to exhibit powerful bipolar jets (Mundt, Brugel, & Bührke 1987), it is clear that the possible effects of outflows on the dusty envelopes need to be considered.

In this paper we assume that the wind-driven holes are bipolar conical cavities of opening half-angle at infinity θ_0, measured from the polar (rotational) axis. The schematic geometry of our model is shown in Figure 2. The idea behind this simple model is that the wind completely evaculates material inside this cone, leaving the material outside the cone undisturbed. This model may not be realistic but we adopt it in the absence of much definite knowledge of jet geometry. Material just outside this cone has finite angular momentum, and so it will not land on the star but on the disk, at a distance given by

$$\frac{R_{\rm min}}{R_c} = \sin^2 \theta_0 \qquad (2)$$

(e.g., Ulrich 1976; Cassen & Moosman 1981). Our conical cavity intercepts the disk at this radius, approximating the streamlines of the infalling material.

2.2. *Radiative Transfer Methods*

We begin as in KCH by calculating the radiative equilibrium temperature distribution from the *spherical* average of the TSC density distribution (Adams & Shu 1986). We assume that the luminosity originates entirely in the central source, which radiates, isotropically. To minimize the number of parameters we adopt the standard Draine & Lee (1984) dust opacities and assume that dust is destroyed at temperatures $\gtrsim 1600$ K.

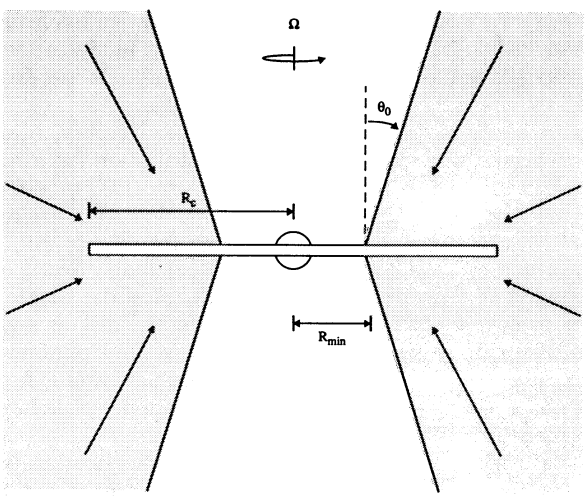

FIG. 2.—Schematic illustration of our axisymmetric envelope model, shown as a cross-cut in the meridional plane. The envelope density distribution is given by the TSC model for rotating collapse (see text), with the same rotational axes for the disk and for the infalling envelope. Material lands on the disk inside of R_c (which value is set by the angular momentum of the envelope). A bipolar outflow is assumed that evacuates the envelope within a cone whose axis lies along the rotational axis, which has an opening angle θ_0, and intersects the disk at $R_{\rm min}$.

The presence of holes in our models introduces substantial departures from spherical symmetry. We tried therefore to make an approximate temperature correction to treat this. At each point of the envelope in the spherically averaged calculation, we split the mean intensity J at each frequency into two pieces,

$$J_\nu = J_{d,\nu} + J_{*,\nu} , \qquad (3)$$

where $J_{d,\nu}$ is the contribution from the dust envelope and $J_{*,\nu}$ is the direct stellar contribution. For envelope models with holes, we assume that J_d is the same as in the spherical calculation, but recalculate the direct stellar contribution

$$J_{*,\nu} = \int d\Omega\, I_{*,\nu} e^{-\tau}/4\pi , \qquad (4)$$

where τ is the optical depth through the envelope toward the star, including the cavity and the actual TSC density distribution, and the integral over solid angle Ω is taken over the stellar disk. With a new estimate of the mean intensity, the temperature is recalculated using the radiative equilibrium equation,

$$\int_0^\infty d\nu\, \kappa_\nu (J_\nu - B_\nu) = 0 , \qquad (5)$$

where B_ν is the Planck function. This approximation results in temperature distributions that approach the spherical distribution far from the cavity, but that are much hotter along the walls of the cavity because of the enhanced penetration of light from the central source.

It must be emphasized that this correction to the temperature distribution for the pressure of a hole is approximate. We shall restrict ourselves to considering only narrow holes, for which the departure from overall spherical symmetry in the envelope is minimized. The temperature rise along the edges of the cavity somewhat enhances the emission at shorter wavelengths, but the final results are dominated by the removal of hot dust from the cavity, which results in less short-wavelength emission overall (see § 3). We assume that the adjusted source function is the Planck function, which also tends to reduce the short-wavelength emission due to the neglect of scattering.

The resulting axisymmetric (but not spherically symmetric) temperature distribution then provides the source function to obtain the emergent spectrum at a given inclination angle i from the formal solution of the transfer equation, as in KCH.

The infall pattern of the TSC model implies the formation of a disk. For the model envelopes of interest here, which permit the escape of short-wavelength light either because of low opacity or the evacuated hole, it is necessary to consider the effect of the disk and its emission on the SED. We assume that the disk is optically thick at all wavelengths, so that it blocks the envelope radiation behind it, with an outer radius of R_c. The radiative equilibrium calculation includes the angle-averaged disk contribution to the total system luminosity (equivalently, we assume that the disk emits isotropically a flux that corresponds to 60° inclination). For simplicity this luminosity is assumed to originate at the star. This is reasonable, since we assume the standard temperature distribution for

steady disk accretion relation (LBP),

$$T_d^4(R) = \frac{3GM\dot{M}}{8\pi\sigma R^3}\left[1 - \left(\frac{R_*}{R}\right)^{1/2}\right], \quad (6)$$

where R is the radial distance in the disk plane, and R_* is the stellar radius; this implies that most of the energy is radiated in the inner disk. The emergent spectrum at inclination angle i is calculated assuming isotropic radiation from the disk oriented perpendicular to the envelope rotational axis.

3. RESULTS FOR ENVELOPE EMISSION

The six flat spectrum sources discussed by ALS II exhibit nearly constant fluxes in λF_λ between about 3 and 60 μm. Specifically, defining the spectral index s between 3.5 and 60 μm as $\lambda L_\lambda \propto \lambda^s$, the ALS II flat spectrum sources have $-0.6 \lesssim s \lesssim 0.4$. In this section we investigate the parameter range in which infalling envelopes can produce similarly flat SEDs without including disk emission or scattered light originating from the central object. We consider models with $L = 4$ $L_\odot$, slightly higher than the median stellar luminosity in Taurus (~ 1 $L_\odot$; Kenyon et al. 1990), but comparable to the luminosities of the flat spectrum sources we model in detail later. The shapes of the calculated SEDs are insensitive to differences in luminosity of an order of magnitude or less (cf. KCH).

3.1. *Models without Holes or Disks*

We begin by considering how well the simplest models, namely TSC envelopes without bipolar outflow holes or disks, can reproduce flat SEDs in this wavelength range. Figure 3 illustrates the radial temperature distributions for TSC models with $R_c = 70$ A.U., but with different values of log ρ_1. At large radii, the envelope temperature distribution approaches the $T \propto r^{-1/3}$ behavior expected in the optically thin limit (Larson 1972; ALS I; KCH). For the lower-density envelopes also considered in Figure 3, the optical depths are even smaller, so the temperature distribution approaches the optically thin limit even more closely. These relatively flat temperature distributions are essential to producing a large far-infrared excess.

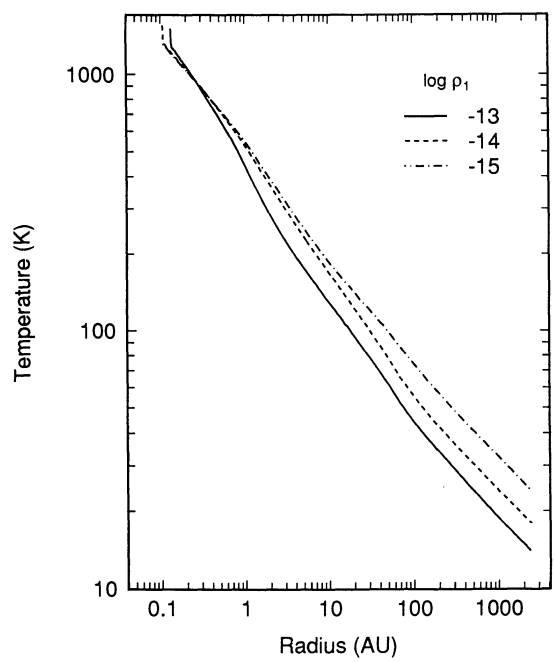

FIG. 3.—Temperature distributions for the TSC infall models without bipolar holes, labeled by the reference level density ρ_1.

The upper panel of Figure 4 illustrates the behavior of the envelope emission as a function of ρ_1 and R_c. At high densities (high infall rates), the SED is relatively narrow; most of the energy comes out in the far-infrared, because the cold outer envelope strongly extincts the shorter-wavelength light. However, for $\rho_1 = 10^{-14}$ g cm^{-3} and $R_c = 70$ AU (shown at $i = 60°$), the spectral energy distribution becomes quite broad, and the 10 μm silicate feature nearly disappears. The infall rates for these two models span the typical values found for many Taurus Class I "protostars" (KCH, KWGH). At $\rho_1 = 10^{-15}$ g cm^{-3} the central star (assumed in these calculations to be a 3500 K blackbody) can be seen clearly, being only slightly extincted by the envelope.

The lower panel of Figure 4 shows the importance of R_c in producing a broad SED. For spherically symmetric collapse. KCH showed that the SED is extremely narrow for $\rho_1 \gtrsim 3 \times 10^{-14}$ g cm^{-3}. Even for $\rho_1 = 10^{-14}$ g cm^{-3}, a spherically symmetric envelope ($R_c \to 0$) produces a relatively narrow SED. If R_c is increased to 300 AU—near the upper limit expected from the observed rotation of cloud cores (Goodman et al. 1993)—the SED becomes slightly double-peaked, as the spectrum of the central star once again becomes important.

For the high infall rates of Class I sources in Taurus KCH pointed out that the inclination of the model made a large difference in its apparent SED, because of the flattened nature of the TSC density distribution and the large extinction at short wavelengths. For more optically thin envelopes, one

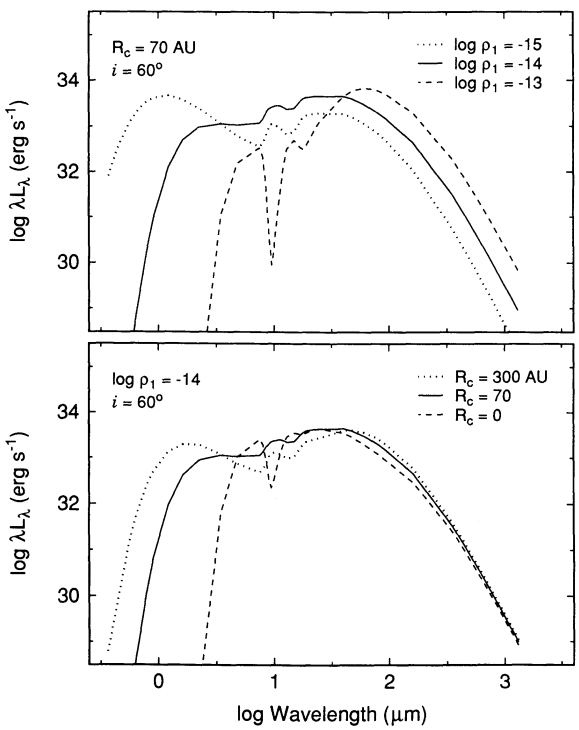

FIG. 4.—SEDs for TSC models without bipolar holes or disks, illustrating the dependence of the emergent flux on the reference level density ρ_1 for a centrifugal radius $R_c = 70$ AU and the effect of varying the centrifugal radius R_c at $\rho_1 = 10^{-14}$ g cm^{-3}.

would expect that the inclination dependence of the SED should become less important. This is explicitly demonstrated in Figure 5, where we show the inclination dependence for two models.

The sequence of models in Figures 4 and 5 show that infall models produce relatively broad and flat SEDs provided the envelope density and optical depth lie within a limited range. For very low infall densities, the central star is not sufficiently obscured and the envelope emission becomes too weak with respect to the short-wavelength peak. For very high infall densities, insufficient near-infrared emission escapes. To a certain extent, changes in ρ_1 can be compensated for by appropriate changes in R_c and i. But there are limits to this scaling, because the wavelength of the peak of the far-infrared SED depends upon ρ_1 (cf. KCH).

Our "fiducial" model with $\log \rho_1 = -14$, $R_c = 70$ AU, $i = 60°$ produces a spectral index between 3.5 and 60 μm of $s = 0.35$. The same model observed at $i = 30°$ results in $s = 0.28$, while at the same density and inclination but $R_c = 300$ AU, $s = 0.39$. These models lie at the upper range of s considered by ALS II. Thus, infall models can explain the mid- to far-infrared emission of the flat spectrum sources with the largest infrared excesses. In fact, some of the Class I sources listed in these papers would fall into that spectrum category if defined by this range of s (specifically, IRAS 04295+2251 and IRAS 04489+3049).

3.2. *Thermal Emission Models with Holes*

We next consider the effects of bipolar cavities on the thermal emission from the infalling envelope. (Note that scattering is not included in these calculations.) Figure 6 shows models with $\rho_1 = 3 \times 10^{-14}$ g cm^{-3}, $R_c = 200$ AU, and with hole sizes of $\theta_0 = 0°$, 5°, 10°, and 30°. The principal effect of the hole at high inclinations is to remove mid-infrared emission, because the inner hot dust of the original TSC model has been removed. A conical hole with $\theta_0 = 10°$, has a distance of closest approach to the star $r_{min} = 0.03R_c = 6$ AU; thus the hole removes the dust with temperatures in excess of ~400 K (see Fig. 2). The flux from the envelope is thus reduced at wavelengths shorter than $\lambda \sim 0.3/T_{max} \sim 8$ μm.

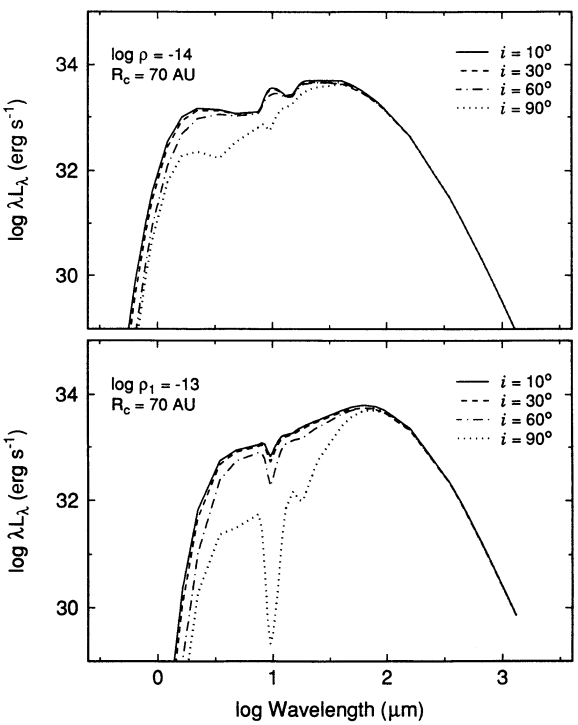

FIG. 5.—Dependence of two TSC model SEDs on the inclination of the pole to the line of sight. Both panels show results for $i = 0°$, 30°, 60°, and 90°, with the uppermost curve indicating $i = 0°$ and the lowermost curve representing $i = 90°$.

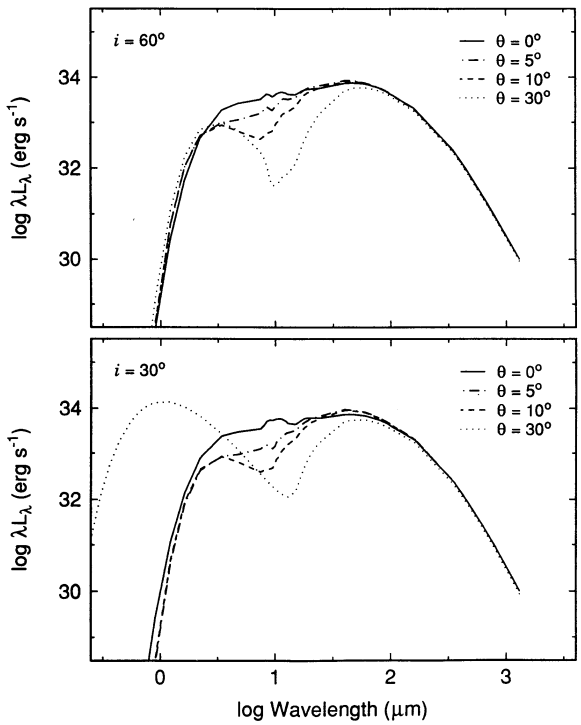

FIG. 6.—Effects of bipolar outflow holes on the SED of a TSC model with $\log \rho_1 = -13.5$, $R_c = 200$ AU. Results are shown for two inclinations, $i = 60°$ (*upper panel*) and 30° (*lower panel*). The dotted lines show the TSC model SED with no bipolar outflow hole; the solid, dashed, and long-dashed lines represent models with half-opening angles for the outflow holes of 0°, 5°, 10°, and 30° (see eqs. [2] and § 2).

Similar results are obtained at low inclinations except when $i \lesssim \theta_0$. In this case the central regions are not affected by extinction along the line of sight, resulting in very strong emission at short wavelengths. The resulting SED is dominated by the emission of the star and disk at short wavelengths and does not look like a flat spectrum source. In the context of the TSC model, flat spectrum sources either require outflow holes with very small opening angles, or an additional source of near- to mid-infrared emission.

3.3. *Summary*

Summarizing the results of this section, we find that TSC infall models without disk emission and with small outflow holes can explain the largest mid- to far-infrared emission observed in flat spectrum sources. The required envelope parameters—$\rho_1 \sim 1$–10×10^{-14} g cm^{-3} and $R_c \sim 70$–300 AU—lie in the range found by KCH and KWGH in their modeling of Class I Taurus sources.

The thermal emission from TSC models produces excess emission with $s \gtrsim 0.3$. To obtain $s \lesssim 0$ it is necessary to consider other sources of emission, especially at shorter wavelengths. In principle, this is not a major difficulty. Since the flat

spectrum sources are optically visible, the detailed spectrum of the central source will affect the resulting SED. Disk emission is a plausible source of extra near-infrared emission, and it is clear from the large polarization exhibited at short wavelengths by objects like HL Tau that geometry-dependent scattering is also important (e.g., Whitney & Hartmann 1993; KWGH).

4. MODELS FOR SPECIFIC OBJECTS

Next we demonstrate that inclusion of disk emission and scattering in bipolar holes allows us to improve the comparison between theory and observations at optical and near-infrared wavelengths. We emphasize, however, that our disks have standard temperature distributions, and that envelope emission dominates in the mid- to far-infrared regions.

We consider in detail two objects which represent extreme examples of the flat spectrum sources studied by ALS II. HL Tau has the largest extinction of the sample, with a very flat SED out to nearly 100 μm. T Tau has one of the lowest extinctions of the group discussed by ALS II, but it has very large far-infrared emission. T Tau is also known to be a binary, and there is now much more information on the relative contributions of the two sources than was available at the time ALS II was written. Our models for these objects assume that HL Tau is not seen along the bipolar flow hole, since it is highly extincted. In contrast, we find that T Tau can best be explained if we assume that we are viewing it along the outflow hole.

4.1. *HL Tau*

HL Tau is a strong-emission object of the "classical" T Tauri type (see Cohen & Kuhi 1979), with strong excess emission at both optical-ultraviolet and infrared wavelengths. The optical spectrum of HL Tau is dominated by strong emission lines and "veiling" continuum. The nature of the central star in HL Tau is uncertain, although it is probably a low-mass object given the modest luminosity of the system, most of which does not appear to arise from the stellar photosphere. This excess luminosity of the strong-emission T Tauri stars is generally supposed to be produced by rapid disk accretion (KH; Bertout et al. 1988; Basri & Bertout 1989). HL Tau has a high-velocity, highly collimated optical jet (Mundt et al. 1987, 1990) situated in the midst of an optical and near-infrared scattered-light nebula that can be traced thousands of AU away (e.g., Gledhill & Scarrott 1989).

Both Beckwith et al. (1989) and Grasdalen et al. (1989) have previously suggested that HL Tau has an infalling envelope. Grasdalen et al. observed redshifted C_2 absorption lines in the 8800 Å region, with velocities ~ 20 km s^{-1}. Beckwith et al. suggested that the near-infrared scattered light from HL Tau came from an envelope, based on the morphology of the nebula, and estimated at a mass infall rate of $\sim 3 \times 10^{-6}\ M_\odot$ yr^{-1}. Recently Hayashi et al. (1993) have suggested that a flattened gaseous disk around HL Tau is falling in at $\sim 5 \times 10^{-6}\ M_\odot$ yr^{-1}.

As discussed in § 1 (Fig. 1), an infalling envelope model with $\log \rho_1 = -13.5$ and $R_c = 70$ AU produces a SED that is similar to that observed in HL Tau at long wavelengths, but does not produce enough emission at short wavelengths. In the context of the TSC model, the far-infrared emission is more sensitive to ρ_1, while the amount of near-infrared light escaping is enhanced by increasing R_c (see KCH). We therefore initially calculated models with the same ρ_1 but larger R_c.

Figure 7 shows that models with $\log \rho_1 = -13.5$, $R_c = 200$ AU, and a central star with a blackbody temperature of 3500 K, can produce a reasonable fit between ~ 10 and ~ 100 μm, as long as the inclination is not much greater than 60°. The inner optical depth depends upon the product $\rho_1 \times R_c^{-1/2}$, so to some extent one can compensate for a higher density with a larger centrifugal radius. This is demonstrated in the bottom panel of Figure 4, although the low-density model can probably be rejected since its peak is at shorter wavelengths than indicated by the observations. (It should be noted that the *IRAS* fluxes are measured with beamsizes that include both HL Tau and its near neighbor XZ Tau. We assumed that HL Tau is twice as bright as XZ Tau in the *IRAS* bands, in the same proportion as the ground-based 10 and 20 μm fluxes.)

The standard infall models come gratifyingly close to explaining the overall shape of the SED, particularly explaining the large far-infrared excess that is so difficult to explain with disk models. However, none of the infall models produce enough emission at $\lambda < 3$ μm. In addition, the CVF photometry of HL Tau by Cohen (1980) indicates a modest silicate absorption feature, whereas the models suggest weak silicate emission.

A more realistic model for HL Tau should include outflow holes, since the jet should be powerful enough to produce a cavity in the envelope (Mundt et al. 1990). It is also necessary to introduce some additional envelope asymmetry to explain the observed reflection nebula (compare Gledhill & Scarrott 1989 with TSC model results without holes in Whitney & Hartmann 1993). We tried a model with a hole of $\theta_0 = 10°$, which could be consistent with the highly collimated jet.

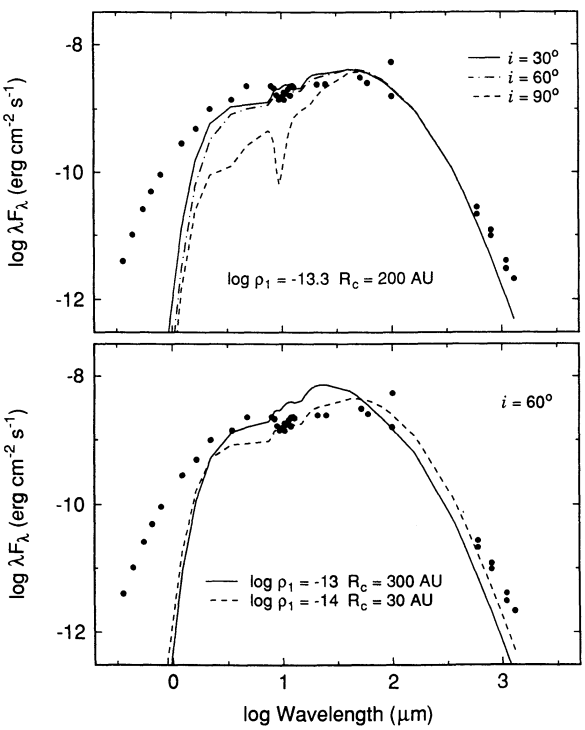

FIG. 7.—Comparison of TSC models with the SED of HL Tau. The log $\rho_1 = -13.5$, $R_c = 200$ AU models do reasonably well at explaining the SED for wavelengths longer than $\lambda \gtrsim 10$ μm, as long as the inclination is not too large. At short wavelengths the observations indicate more emission than the simple TSC models can provide. Note that the model predicts that if HL Tau were viewed nearly equator-on, it would be identified as a Class I source.

As shown in Figure 6, the inclusion of the cavity substantially reduces the envelope emission shortward of 10 μm. Within the context of the conical hole model the near-infrared emission must come from the disk.

We obtained the best fit to the near infrared spectrum with a disk that has a steady accretion disk temperature distribution (eq. [6]) and a central hole (in the disk) of $\sim 7R_*$, with $R_* = 3$ $R_\odot$. The final model is shown in Figure 8. To obtain the flux in the near-infrared, most of the luminosity must be accretion luminosity. In this model one third of the system luminosity is emitted by the disk, while the other two thirds of the luminosity must be emitted by a hot component. We assume that the hot component has a temperature of 10,000 K. The thermal emission from the envelope SED is not sensitive to the assumed temperature of the hot component, since this short-wavelength radiation is effectively absorbed by the envelope. However, the optical radiation is sensitive to the choice of temperature.

The thermal-equilibrium model calculations do not include scattering of short-wavelength light. On the other hand, the high polarization observed at $\lambda \lesssim 2$ μm indicates that optical and near-infrared emission is mostly scattered light from the central source (Hodapp 1984; Bastien 1985). Using the same envelope parameters, conical hole size, and input source spectrum as those assumed in the radiative equilibrium calculations, and the methods and standard dust properties described in Whitney & Hartmann (1992, 1993) and KWGH, we calculated the scattered flux in the optical and near infrared shown in Figure 8 (open circles); it agrees remarkably well with the observations. The optical radiation is sensitive to the temperature of the hot component, given a fixed system luminosity.

The results of the modeling of the optical and near-infrared emission are at best tentative, given all the parameters involved, and are certainly not unique. However, the basic idea for the physics of the situation is not without precedent. Stellar magnetospheres that hold off T Tauri disks from the central star are increasingly invoked to explain observations (Bertout et al. 1988; Königl 1991; Calvet & Hartmann 1992; Bouvier et al. 1993; Edwards et al. 1993). Bertout et al. (1988) found that they could not model DR Tau, a strong-emission T Tauri star like HL Tau (see Cohen & Kuhi 1979), without stopping the disk at about three stellar radii. Kenyon et al. (1994) have arrived at a similar conclusion and furthermore conclude that most of the accretion energy is liberated as the infalling material in the magnetosphere shocks against the stellar photosphere. The strong excess emission of HL Tau at optical-ultraviolet wavelengths relative to the stellar photosphere is generally interpreted to mean that the accretion luminosity is much bigger than the stellar luminosity (KH; Bertout et al. 1988; Basri & Bertout 1989), as we have assumed in this particular model.

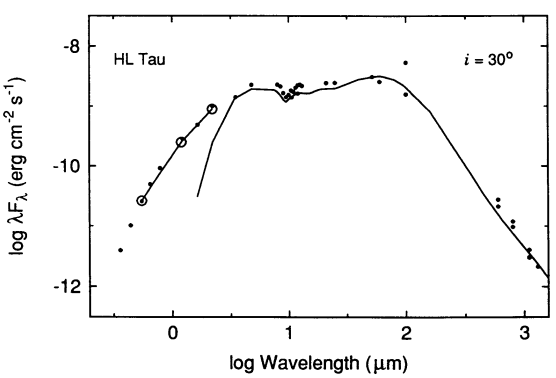

FIG. 8.—Comparison of a TSC model (*solid line*) with log $\rho_1 = -13.5$, $R_c = 200$ AU (see Fig. 7) but now including a bipolar cavity of opening angle $\theta_0 = 10°$ and disk emission (see text). The inclusion of the hole and the disk near-infrared emission now enables the fit to be made to the mid-infrared emission, for wavelengths $\lambda \gtrsim 3$ μm, and also produces a silicate absorption feature in better agreement with observations. Scattered light calculations (*open circles*) show that the model can also explain the optical and near-infrared emission with a hot central source and enhanced scattering because of the bipolar cavity (see text).

Interestingly, the inclusion the inclusion of disk emission changes the silicate feature from emission to absorption, in better agreement with observations. This occurs because part of the envelope is now seen in projection against the bright disk. Our modeling suggests that the appearance of the silicate feature could be quite sensitive to disk accretion rate and geometry in addition to the infall rate.

Our model envelope has an infall rate remarkably consistent with the estimate of Beckwith et al. (1989). The central mass is not accurately known, but adopting 0.5 $M_\odot$ results in $\dot{M} \sim 4 \times 10^{-6}$ $M_\odot$ yr^{-1}, almost identical to the Beckwith et al. estimate, and comparable to the Grasdalen et al. (1987) and Hayashi et al. (1993) estimates. Moreover, our results show that the infalling envelope required by Beckwith et al. to explain the near-infrared scattering *must* produce very large infrared emission, comparable to that which is observed, *if* the envelope extends to a few thousand AU. Beckwith et al. did not come to this conclusion because the scattered light could only be seen to a distance of a few hundred AU in their data, but the envelope must be much larger than this, as indicated by the deeper images (e.g., Gledhill & Scarrott 1989).

The ~ 20 km s^{-1} redshift of C_2 lines found by Grasdalen et al. (1989) suggests that material is falling in quite close to the central star, to distances of no more than a few AU. If this observation is correct, it supports our model requirement that dust fall in quite close to the central source to produce sufficient mid-infrared envelope emission. In the model shown in Figure 7, the closest dust to the star is at $R_{env} \sim 6$ AU. The free-fall velocity at this distance is $\sim 14(M/0.5\ M_\odot)^{1/2}$ km s^{-1}, so we might need to modify our model to have an even smaller R_{env}, especially considering projection effects. (Note that the presence of infall to such small distances suggests that the jet is highly collimated and comes from the very innermost disk; otherwise this infalling material would presumably be blown away.)

As pointed out by Whitney & Hartmann (1993), infalling dusty envelopes, having cavities and infall rates and R_c comparable to those adopted here, can produce high polarization such as observed in HL Tau. An opaque envelope can extinct the unpolarized light from the central star much more than the highly polarized scattered light from the extended nebula. Moreover, Whitney & Hartmann (1993) showed that envelope + cavity models tend to produce a net polarization perpendicular to the disk axis; in contrast, disk models generally produce polarization parallel to the disk axis (Whitney & Hartmann 1992). In the case of HL Tau, the net polarization of the central source is perpendicular to the jet (Hodapp 1984), so that if we assume the jet is along the disk axis, the observations are more consistent with the envelope model than with the disk scattering model. More discussion of the scattered light nebula and polarization of HL Tau will be presented in a forthcoming paper (Whitney et al. 1994).

HL Tau emits strongly at mm wavelengths from a region $\lesssim 190$ AU at 2.7 mm; Sargent & Beckwith (1987, 1991) and Beckwith et al. (1990) attribute this emission to a relatively massive disk. Our model envelope contains very little mass on this scale and so cannot explain this unresolved millimeter emission.

In summary, we find that an infalling envelope model can fit the mid- to far-infrared SED of HL Tau. Moreover, the SED model is *quantitatively* consistent with completely independent observations supporting the infall picture. Disk emission is probably required to explain the *near-infrared* emission (as well as the mm emission), and enhanced scattering due to a hole in the envelope is required to explain the optical emission.

4.2. *T Tau*

T Tauri has been recognized as a binary system for several years (Dyck, Simon, & Zuckerman 1982; Schwartz et al. 1984; Schwartz, Simon, & Campbell 1986; Ghez et al. 1991) and is an example of the class of T Tauri stars with optically invisible, infrared-bright companions. The detailed speckle measurements of Ghez et al. (1991) distinguish the separate fluxes of the two components between 1.3 and 12 μm. The infrared-bright T Tau S is quite variable; for this object we show the fluxes at the latest epoch ($\sim$1990) in Figure 9.

It is evident from these observations that both objects exhibit substantial excess infrared emission. At optical wavelengths T Tau N undoubtedly dominates the emission. The situation at far-infrared wavelengths is much less clear. T Tau S appeared much fainter at the epoch ($\sim$1983) of the *IRAS* flux measurements (Ghez et al. 1991), and so it may be that the far-infrared emission shown in Figure 9 was mostly powered by the optical star. We assume this in the analysis that follows.

The summed emission of the optical star and the infrared companion produces a SED that is naturally flatter than those of the individual components. ALS II noted the presence of the infrared companion, but argued that the combination of two separate sources would be very unlikely to add up so nicely over such a large wavelength interval. However, each individual source in T Tau has a much broader SED than a single-temperature blackbody. Because T Tau N is optically visible, with little apparent extinction (Cohen & Kuhi 1979), the intrinsic spectrum of this source is fairly well known, and it seems likely that the near-infrared excess of the optical object arises in a circumstellar disk (KH).

An infalling dusty envelope in the T Tau system has been invoked by Weintraub et al. (1992) and Whitney & Hartmann (1993) to explain the near-infrared scattered light. Weintraub et al. suggested that the surrounding nebula must depart from spherical symmetry to reconcile the scattered light distribution with the low visual extinction to the optical component. Whitney & Hartmann explicitly suggested that the low A_V is due to a wind-driven hole along the line of sight, since T Tauri is probably observed nearly pole-on (Herbst et al. 1986).

Figure 9 (upper) shows a comparison between T Tau N (the optical star) and an envelope model with $\rho_1 = -14$, $R_c = 100$ AU (compare also Fig. 6.) We have included a hole of opening angle 20°, and have assumed that the inclination to the line of sight is almost zero, that is, that we are looking down the hole. The central source of the model is a star with $T_{\rm eff} = 5000$ K and $R = 3.5\ R_\odot$, surrounded by a steady accretion disk that emits 10% of the luminosity of the system. Another 10% is emitted in a hot component, which accounts for the ultraviolet excess (KH).

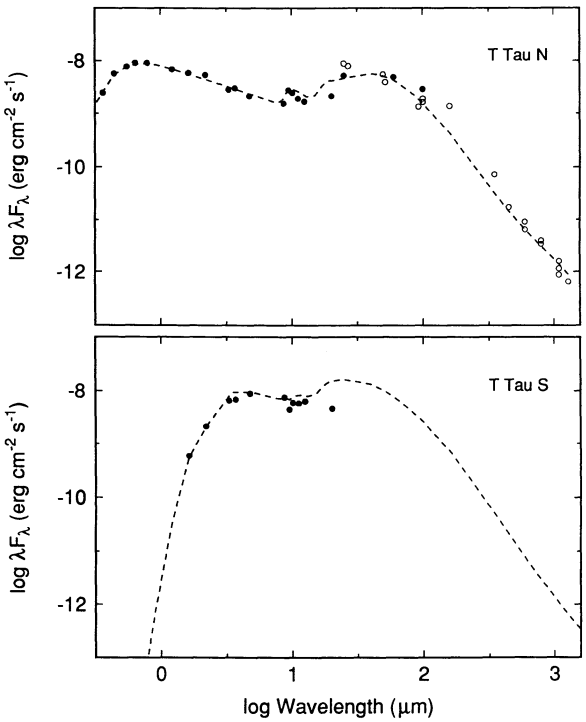

FIG. 9.—(*upper panel*) T Tau N SED compared to TSC models with bipolar holes and disk. The data for 2 μm $\leq \lambda \leq$ 20 μm are taken from the speckle interferometry of Ghez et al. (1991). It is assumed that all of the optical light arises from T Tau N. We also associate the far-infrared *IRAS* and KAO observations with T Tau N, although this emission arises on scales much larger than the binary, because the historical information on the variability of T Tau S indicates that it was much fainter during these observations (see text). The dashed line is a model $\log \rho_1 = -14$, $R_c = 100$ AU, with a bipolar cavity of opening angle $\theta_0 = 20°$. Disk emission is included in the model, which explains the infrared emission at wavelengths <10 μm; the disk is taken to have a standard temperature distribution with radius (see text). The envelope emission produces the silicate emission feature and dominates the continuum at long wavelengths (*lower panel*). The SED of T Tau S, taken from the speckle observations of Ghez et al. (1991) near maximum light. The model (*dashed line*) is shown for the same ρ_1 as used for T Tau N, but with $R_c = 30$ AU and no bipolar outflow hole (see text).

The infalling envelope contributes most of the flux at wavelengths $\gtrsim 10$ μm. The envelope does not need to come as close to the central star as in the case of HL Tau to explain the infrared spectrum, since the disk dominates in the wavelength region $\sim$2–10 μm. Our model disk has the standard Lynden-Bell & Pringle (1974) temperature distribution.

The silicate feature is in emission in the model. This emission was observed by Ghez et al. (1991) in T Tau N. We find that 90% of the flux in the silicate emission arises within 30 AU $\sim$0.″2 of the optical star. This seems to be consistent with the slit scans of Ghez et al. (1991), which appear to have had a FWHM resolution $\sim$0.″5.

Infall in a binary system must have a much more complicated density structure than can be predicted by the simple TSC model (see, e.g., the discussion in Bonnell & Bastien 1992). However, since the far-infrared emission must be produced in a circumbinary envelope, envelope material must be falling toward T Tau S as well. The bottom panel of Figure 9 shows a comparison of T Tau S with an infall model with the same ρ_1 but with a smaller $R_c = 30$ AU. Note that one can obtain silicate absorption instead of emission with the same infall rate, pointing out the importance of geometry in the appearance of

the silicate feature. The comparison suggests that the infalling envelope is a viable model for T Tau S, although our simple model geometry prevents us from making more than an approximate comparison.

Our suggested picture for the T Tau system is that the central stars are surrounded by a circumbinary infalling envelope which is responsible for the far infrared excess. The line of sight to T Tau N is relatively clear, and so we see basically the star plus disk, along the excess at $\lambda \gtrsim 10$ μm from the infalling envelope. For some reason the line of sight to T Tau S is more extincted. Although the situation must be complex, we suggest that this observation can in principle be explained by an infalling envelope which has a centrifugal radius of the order of the 100 AU projected binary separation. If the components are of unequal mass, then one component might be more visible to us because it is closer to the system center of mass, and thus possibly more aligned with the outflow hole. Clearly further examination of this problem will require more sophisticated dynamical calculations. For the moment, it is encouraging that T Tau S can be fitted with the same ρ_1 as T Tau N, which is to be expected if both are necessarily situated within a common infalling envelope.

Note also that if we adopt a central mass of 2 $M_\odot$ (cf. Cohen & Kuhi 1979), then even by adopting a somewhat lower value of $\log \rho_1 = -14$ the mass infall rate, 2.7×10^{-6} $M_\odot$ yr^{-1}, is right at the median for Class I Taurus sources.

The case for the infalling envelope model in T Tau S is strengthened by the lack of plausible alternatives. Another model, suggested by Ghez et al. (1991), is that T Tau S is a rapidly accreting disk. Ghez et al. show that such a model can reproduce the SED of T Tau S reasonably well. They further note that this object has been quite variable in the past few years, and suggest that it might be a type of FU Orionis object.

One difficulty with a pure disk model is the low peak temperature, which implies a very large inner radius. To see this, note that the maximum temperature of a steady accretion disk is

$$T_{\max} = 0.488\left(\frac{3GM\dot{M}}{8\pi R_*^3\sigma}\right)^{1/4}, \tag{7}$$

and since the accretion luminosity of the disk is

$$L_d = \frac{1}{2}\frac{GM\dot{M}}{R}, \tag{8}$$

$$T_{\max} = 0.488\left(\frac{3L_d}{4\pi R_*^2\sigma}\right)^{1/4} = 1140\ \mathrm{K}\left(\frac{L_d}{8\ L_\odot}\right)^{1/4}\left(\frac{R_*}{30\ R_\odot}\right)^{-1/2}. \tag{9}$$

As pointed out by Ghez et al., to explain the low temperature of the disk without invoking much more extinction toward the southern than the northern component, it is necessary to assume that the inner radius of the disk is $R \gtrsim 30$ $R_\odot$ at maximum light. This inner radius is very large in comparison with the typical radii of T Tauri stars $R_* \sim 2$–3 $R_\odot$ and the inner disk radii of well-studied FU Ori objects ($R_i \sim 5$ $R_\odot$). Although magnetospheres may hold T Tauri disks off the surface of the star to substantial distances, as we have assumed for HL Tau, it is worrisome to invoke a magnetospheric radius as large as ~ 15 R_* (Camenzind 1990; Königl 1991).

The strongest argument against the pure disk model involves the change in luminosity of T Tau S between 1986 and 1991 of nearly a factor of 10. For a constant inner radius the disk model would predict an increase of nearly 1.8 in the maximum temperature of the disk, while the observations indicate a constant $T_{\max}$ or perhaps even a slight decrease at high luminosity. As Ghez et al. point out, the inner disk radius could change; but if the inner inner radius is determined by a magnetosphere, then one would expect the magnetosphere to shrink under the impact of a higher accretion flow. This would produce an even larger change in the maximum temperature.

On the other hand, the absence of any large change in the peak wavelength of the SED with increasing luminosity is much more simply explained with an infalling envelope model. As shown by KCH, the peak of the SED for dusty envelopes changes very slowly with luminosity ($\lambda_{\max} \approx L^{1/12}$ at long wavelengths), more consistent with the observed absence of color variations.

T Tau S may well be an accretion disk *embedded* within an infalling envelope. As suggested by Ghez et al., the variability of this source may best be explained in the context of variable disk accretion. In this case, the infall of material may feed the disk and help produce events of rapid accretion (Kenyon & Hartmann 1991).

5. DISCUSSION

The results of the previous section show that infalling envelope models can reproduce the mid- to far-infrared emission of flat spectrum T Tauri stars. The infall rates needed are precisely those predicted by theory (e.g., Shu 1977; Stahler, Shu, & Taam 1980). Moreover, observations of Class I sources suggest the same infall rates (ALS; Butner et al. 1991; KCH; KWGH). Thus, the infall model is situated solidly in the context of the current picture of star formation. Moreover, because the infall rates are the same for other objects regarded as "protostars," young objects still to acquire substantial amounts of mass from their infalling envelopes, it seems quite likely that some of the flat spectrum sources are protostars as well.

The models demand that the infalling material land directly on a disk. Disks are therefore an essential component of the infall picture. Disk emission may need to be taken into account, particularly at short wavelengths. On the other hand, these disks do not need to have nonstandard temperature distributions. The envelope most naturally explains the mid- to far-infrared emission. The ultimate energy source is, as expected, situated deep in the gravitational potential well, and the envelope serves merely as a mechanism for converting this energy to long-wavelength radiation. The simplicity and power of this explanation indicates that models employing "active" disks, in which the temperature distribution is a parameterized power law, should be invoked with caution.

Another attraction of the infall picture is that it can naturally explain the extended reflection nebulae of objects such as T Tau and HL Tau (Whitney & Hartmann 1993), whereas disk models have difficulties in explaining the morphologies and polarization patterns of these nebulae (Whitney & Hartmann 1992). Indeed, infall was originally suggested for both of these particular objects as a means of explaining the observed scattered light (Beckwith et al. 1989; Weintraub et al. 1992).

Our models predict the existence of a dusty envelope on scales of thousands of AU around flat spectrum sources. In the case of HL Tau, Sargent & Beckwith (1987, 1991) discovered an elongated structure in ^{13}CO of extent $\sim$3000 AU at a position angle very nearly perpendicular to the optical jet.

The morphology and kinematic behavior of this structure originally suggested a rotating Keplerian disk seen nearly edge-on. The scale of this disk is apparently inconsistent with our models; it is comparable to our envelope dimensions, rather than our disk. However, Hayashi et al. (1993) have recently interpreted this extended molecular material as a gaseous disk, but one in which the material is not centrifugally supported; the dominant motion is infall, not rotation. It is tempting to suggest that this material might correspond to our infalling envelope, but our envelope cannot be a highly flattened disk; there would not be enough far-infrared emission, because the envelope would subtend too small a solid angle to explain the observed far-infrared luminosity. For the same reason, the scattered light from a very flattened structure would be much fainter than for the less flattened envelope we envision.

Galli & Shu (1993a, b) have pointed out that magnetic fields might play a role in flattening an infalling envelope, and suggest that the HL Tau observations might indicate the formation of a "pseudodisk," in which part of the gas falls in to form a nonrotationally supported, infalling disk, while a more extended halo of infalling gas, in a more nearly spherical distribution, is also falling in. Perhaps further studies of the optical and near-infrared scattered light, which emerges over a region comparable to "extended gaseous disk," can help resolve this issue.

Another question is the structure of bipolar flows and the holes that they must produce in the surrounding dusty envelope. As shown above, if bipolar holes are too large, the envelope will not produce enough near- to mid-infrared emission, which must in consequence be accounted for by disk emission (or possibly by envelope emission from an infrared companion). On the other hand, the observations of 20 km s^{-1} redshifts in the C_2 lines of HL Tau by Grasdalen et al. (1989) suggest that material manages to fall in as close as ~ 1 AU. Clearly this important observation should be reconfirmed and extended if possible, since it bears directly on the question of envelope emission at short wavelengths.

Finally, if flat-spectrum sources are produced by infall at high rates, then their number should be constrained by the natural timescale of infall. We will defer detailed consideration of this point to a later paper, but note here that the number of such sources in Taurus (which depends somewhat on the exact definition of the class) is a modest fraction of the known Class I sources. This is consistent with the basic infall hypothesis, since an optically selected sample of objects with substantial infall must be biased toward objects with large R_c or favorable inclinations to the line of sight, and these should not be the majority of the infall sources.

6. CONCLUSIONS

We have shown that emission from infalling dusty envelopes around T Tauri stars provides an attractive explanation of the SEDs of flat spectrum sources, without recourse to "flat spectrum" disks with unknown physics. We are able to reproduce mid- to far-infrared SED of HL Tau with a dusty infalling envelope in radiative equilibrium, adopting essentially the same mass infall rate as that independently estimated from observations of scattered light and redshifted absorption. We are also able to explain the far-infrared excess of T Tau N, adopting a similar infall model as in HL Tau, but observing the system along an evacuated bipolar cavity. The infall model is also consistent with models constructed to explain the scattered light nebula of T Tau, and probably can explained the main features of the SED of the infrared companion T Tau S. For both systems, disk emission is required to explain the near-infrared and millimeter wavelength fluxes, but the disk may have the standard (i.e., Lynden-Bell & Pringle 1974; ALS) temperature distribution. The infall rates required by models of flat spectrum sources are similar to those required to model Class I sources.

There are several major unresolved issues concerning the infalling envelopes of Class I sources and T Tauri stars. For example, what is the real structure of the envelope? The TSC model is attractive, but if binary formation occurs early on, the remnant envelope could look substantially different (e.g., Bonnell & Bastien 1992; Bonnell et al. 1992). Galli & Shu (1993a, b) have pointed out that magnetic fields might play a role in flattening the envelope, which we have not considered here.

Finally, if infall does not terminate abruptly, but rather decays over a finite interval of time, there could be a period in the evolution of T Tauri stars during which the surrounding envelope is not very opaque, but still affects the far-infrared emission by scattering light into the disk (Natta 1993). We will examine this question further in a subsequent paper.

This work was supported in part by NSF grant INT-9203015, CONICIT grant PI-078, and by NASA grant NAGW-2919.

REFERENCES

Adams, F. C., Lada, C. J., & Shu, F. H. 1987, ApJ, 312, 788 (ALS I)
———. 1988, ApJ, 326, 865 (ALS II)
Adams, F. C., Ruden, S. P., & Shu, F. H. 1989, ApJ, 358, 495
Adams, F. C., & Shu, F. H. 1986, ApJ, 308, 836
Basri, G., & Bertout, C. 1989, ApJ, 341, 340
Bastien, P. 1985, ApJS, 59, 277
Beckwith, S., Sargent, A., Chini, R., & Gusten, R. 1990, AJ, 99, 1024
Beckwith, S. V. W., Sargent, A. I., Koresko, C. D., & Weintraub, D. A. 1989, ApJ, 343, 393
Bertout, C., Basri, G., & Bouvier, J. 1988, ApJ, 330, 350
Bonnell, I., Arcoragi, J. P., Martel, H., & Bastien, P. 1992, ApJ, 400, 579
Bonnell, I., & Bastien, P. 1992, ApJ, 401, 654
Bouvier, J., Cabrit, S., Fernández, M., Martin, E. L., & Matthews, J. M. 1993, A&A, 272, 176
Butner, H. M., Evans, J. J., II, Lester, D. F., Levreault, R. M., & Strom, S. E. 1991, ApJ, 376, 636
Calvet, N., & Hartmann, L. 1992, ApJ, 386, 239
Camenzind, M. 1990, Reviews in Modern Astronomy (Berlin: Springer), 3, 234
Cassen, P., & Moosman, A. 1981, Icarus, 48, 353
Cohen, M. 1980, MNRAS, 191, 499
Cohen, M., & Kuhi, L. V. 1979, ApJS, 41, 473
Draine, B. T., & Lee, H. M. 1984, ApJ, 285, 89
Dyck, H. M., Simon, T., & Zuckerman, B. 1982, ApJ, 255, L103
Edwards, S., et al. 1993, AJ, 106, 372
Galli, D., & Shu, F. H. 1993a, ApJ, 417, 220
———. 1993b, ApJ, 417, 243
Ghez, A. M., Neugebauer, G., Gorham, P. W., Haniff, C. A., Kulkarni, S. R., Matthews, K., Koresko, C., & Beckwith, S. 1991, AJ, 102, 2066
Gledhill, T. M., & Scarrott, S. M. 1989, MNRAS, 236, 139
Goodman, A. A., Benson, P. J., Fuller, G. A., & Myers, P. C. 1993, ApJ, 406, 528
Grasdalen, G. L., Sloan, G., Stout, M., Strom, S. E., & Welty, A. D. 1989, ApJ, 339, L37
Hayashi, M., Ohashi, N., & Miyama, S. 1993, ApJ, 418, L71
Herbst, W., et al. 1986, ApJ, 310, L71
Hodapp, K.-W. 1984, A&A, 141, 255
Kenyon, S. J., Calvet, N., & Hartmann, L. 1993a, ApJ, 414, 676 (KCH)
Kenyon, S. J., & Hartmann, L. 1987, ApJ, 323, 714 (KH)
———. 1991, ApJ, 383, 664
Kenyon, S. J., Hartmann, L. W., Hartigan, P., Strom, K. M., Strom, S. E., Carrasco, L., Recillas, E., & Cruz-Gonzalez, I. 1994, AJ, submitted
Kenyon, S. J., Hartmann, L. W., Strom, K. M., & Strom, S. E. 1990, AJ, 99, 869
Kenyon, S. J., Whitney, B., Gomez, M., & Hartmann, L. 1993b, ApJ, 414, 773 (KWGH)

Königl, A. 1991, ApJ, 370, L39
Lada, C. J., & Wilking, B. A. 1984, ApJ, 287, 610
Larson, R. B. 1972, MNRAS, 157, 121
Lynden-Bell, D., & Pringle, J. E. 1974, MNRAS, 168, 603
Mundt, R., Brugel, E. W., & Bührke, T. 1987, ApJ, 319, 275
Mundt, R., Ray, T. P., Bührke, T., Raga, A. C., & Solf, J. 1990, A&A, 232, 37
Myers, P. C., Fuller, G. A., Mathieu, R. D., Beichman, C. A., Benson, P. J., Schild, R. E., & Emerson, J. P. 1987, ApJ, 319, 340
Natta, A. 1993, ApJ, 412, 767
Rucinski, S. M. 1985, AJ, 90, 2321
Safier, P. 1993a, ApJ, 408, 148
———. 1993b, ApJ, 408, 160
Sargent, A. I., & Beckwith, S. 1987, ApJ, 323, 294
———. 1991, ApJ, 382, L31
Schwartz, P. R., Simon, T., & Campbell, R. 1986, ApJ, 303, 233
Schwatz, P. R., Simon, T., Zuckerman, B., & Howell, R. R. 1984, ApJ, 280, L23
Shu, F. H. 1977, ApJ, 214, 488
Shu, F. H., Tremaine, S., Adams, F. C., & Ruden, S. P. 1990, ApJ, 358, 495
Stahler, S. W., Shu, F. H., & Taam, R. E. 1980, ApJ, 241, 637
Terebey, S., Shu, F. H., & Cassen, P. 1984, ApJ, 286, 529 (TSC)
Terebey, S., Vogel, S. N., & Myers, P. C. 1989, ApJ, 340, 472
Ulrich, R. K. 1976, ApJ, 210, 377
Weintraub, D. A., Kastner, J. H., Zuckerman, B., & Gatley, I. 1992, ApJ, 391, 784
Whitney, B. A., & Hartmann, L. 1992, ApJ, 395, 529
———. 1993, ApJ, 402, 605
Whitney, B. A., et al. 1994, in preparation